



LyeTxI-b, a Synthetic Peptide Derived From *Lycosa erythrognatha* Spider Venom, Shows Potent Antibiotic Activity *in Vitro* and *in Vivo*

Pablo V. M. Reis¹, Daiane Boff¹, Rodrigo M. Verly², Marcella N. Melo-Braga¹, Maria E. Cortés³, Daniel M. Santos⁴, Adriano M. de C. Pimenta¹, Flávio A. Amaral¹, Jarbas M. Resende⁵ and Maria E. de Lima^{1*}

¹ Departamento de Bioquímica e Imunologia, Instituto de Ciências Biológicas, Universidade Federal de Minas Gerais, Belo Horizonte, Brazil, ² Departamento de Química, Faculdade de Ciências Exatas, Universidade Federal dos Vales do Jequitinhonha e Mucuri, Diamantina, Brazil, ³ Departamento de Odontologia Restauradora, Faculdade de Odontologia, Universidade Federal de Minas Gerais, Belo Horizonte, Brazil, ⁴ Serviço de Proteômica e Aracnídeos – Diretoria de Pesquisa e Desenvolvimento, Fundação Ezequiel Dias, Belo Horizonte, Brazil, ⁵ Departamento de Química, Instituto de Ciências Exatas, Universidade Federal de Minas Gerais, Belo Horizonte, Brazil

OPEN ACCESS

Edited by:

Octavio Luiz Franco,
Universidade Católica de Brasília,
Brazil

Reviewed by:

Anirban Bhunia,
Bose Institute, India
César de la Fuente,
Massachusetts Institute
of Technology, United States

*Correspondence:

Maria E. de Lima
melpg@icb.ufmg.br;
lima.mariaelena@gmail.com

Specialty section:

This article was submitted to
Antimicrobials, Resistance
and Chemotherapy,
a section of the journal
Frontiers in Microbiology

Received: 05 December 2017

Accepted: 21 March 2018

Published: 06 April 2018

Citation:

Reis PVM, Boff D, Verly RM, Melo-Braga MN, Cortés ME, Santos DM, Pimenta AMC, Amaral FA, Resende JM and de Lima ME (2018) LyeTxI-b, a Synthetic Peptide Derived From *Lycosa erythrognatha* Spider Venom, Shows Potent Antibiotic Activity *in Vitro* and *in Vivo*. *Front. Microbiol.* 9:667. doi: 10.3389/fmicb.2018.00667

The antimicrobial peptide LyeTxI isolated from the venom of the spider *Lycosa erythrognatha* is a potential model to develop new antibiotics against bacteria and fungi. In this work, we studied a peptide derived from LyeTxI, named LyeTxI-b, and characterized its structural profile and its *in vitro* and *in vivo* antimicrobial activities. Compared to LyeTxI, LyeTxI-b has an acetylated N-terminal and a deletion of a His residue, as structural modifications. The secondary structure of LyeTxI-b is a well-defined helical segment, from the second amino acid to the amidated C-terminal, with no clear partition between hydrophobic and hydrophilic faces. Moreover, LyeTxI-b shows a potent antimicrobial activity against Gram-positive and Gram-negative planktonic bacteria, being 10-fold more active than the native peptide against *Escherichia coli*. LyeTxI-b was also active in an *in vivo* model of septic arthritis, reducing the number of bacteria load, the migration of immune cells, the level of IL-1 β cytokine and CXCL1 chemokine, as well as preventing cartilage damage. Our results show that LyeTxI-b is a potential therapeutic model for the development of new antibiotics against Gram-positive and Gram-negative bacteria.

Keywords: LyeTxI, *Lycosa erythrognatha*, LyeTxI-b, antimicrobial peptide, septic arthritis

Abbreviations: AMPs, antimicrobial peptides; BHI, brain heart infusion; CD, circular dichroism; CFU, colony-forming unit; CHCA, α -cyano-4-hydroxycinnamic acid; Clin, clindamycin; CXCL1, chemokine (C-X-C motif) ligand 1; DME, N,N-dimethyl-formamide; ED₅₀, effective dose 50; ¹H-¹⁵N HMQC, ¹H-¹⁵N heteronuclear multiple quantum coherence; ¹H-¹³C HSQC, ¹H-¹³C Heteronuclear Single Quantum Coherence; Htr, homodimeric peptide homotarsinin; Htr-M, homotarsinin monomeric chain; IL-1 β , interleukin 1 beta; NMR, nuclear magnetic resonance; NOESY, nuclear Overhauser enhancement spectroscopy; MALDI-TOF/TOF, matrix-assisted laser desorption/ionization – time of flight; MBC, minimal bactericidal concentration; mBSA, methylated bovine serum albumin; MH, Mueller-Hinton; MIC, minimum inhibitory concentration; PBS, phosphate buffered saline; POPC, 1-palmitoyl-2-oleoyl-*sn*-glycero-3-phosphocholine; POPG, 1-palmitoyl-2-oleoyl-phosphatidylglycerol; RP-HPLC, reverse phase high-performance liquid chromatography; SDS, sodium dodecyl sulfate; TFE-d₂, 2,2,2-trifluoroethanol-1,1-d₂; TOCSY, total correlation spectroscopy.

INTRODUCTION

Super-resistant bacteria are an emerging public health problem. The urge to develop new tools and strategies to combat the superbugs is clear and was vehemently warned by the World Health Organization in a report about the global threat of antimicrobial resistance, in June 2014 (WHO, 2014). In a majority, this problem is associated with an evolutionary adaptation of bacteria that are found in a multicellular specialized formation called biofilm, which increases the resistance to conventional antibiotics (de la Fuente-Nunez et al., 2013, 2016). Thus, biofilm represents a challenge to treat. In the meantime, AMPs have become a new hope as tools against superbugs, as they are the primary immune defense of animals and can also be found in bacteria, fungi, and plants (Bulet et al., 1999; Ageitos et al., 2017). Although AMPs are less likely to induce resistance in bacteria, there are several studies demonstrating that these molecules induce resistance by multiple mechanisms, as increasing expression of proteases that can cleave the peptide, modifying plasma membrane composition and pump efflux (Nizet, 2006; Andersson et al., 2016). However, recently it has been shown that combination of different phylogenetic taxa AMPs, decrease the evolution of microbial resistance against them (Dobson et al., 2013). In addition, AMPs and derived peptides have shown activity against infections due to biofilm formation (de la Fuente-Nunez et al., 2016).

Antimicrobial peptides are typically composed of 7–44 amino acid residues, usually exhibiting amphipathic alpha helix or beta-sheet conformations and being positively charged (Jenssen et al., 2006; Mookherjee and Hancock, 2007; Dawson and Liu, 2008; Epanand and Epanand, 2011; Wang et al., 2012), although other structural arrangements such as random coil, beta turn, helix-loop-helix, and coiled coil conformations have also been observed (Ghosh et al., 2014; Datta et al., 2015; Verly et al., 2017). Most of the works in literature correlate the activity of these compounds to their membrane-interactions and membrane-disruptive properties (Yang et al., 2001; Bechinger and Gorr, 2017). However, a rising number of works have described the action of the peptides on interactions with intracellular components as DNA, proteins, and also some enzymes (Brogden, 2005; Azim et al., 2016).

A great variety of molecules, such as amino acids, polyamines, proteins, and peptides can be found in spider venoms, including *Lycosa erythrognatha*. In particular, the venom peptides can interact with ion channels and cell receptors, and some of them show antimicrobial activity (Santos et al., 2016). Most of the investigations on AMPs isolated from spiders have proved the activity of several of these compounds against planktonic bacteria or fungi, although many studies have also shown their activities against bacteria biofilms (Overhage et al., 2008; Ageitos et al., 2017).

Our group previously isolated and characterized a new peptide, named LyeTxI, from the venom of the spider *Lycosa erythrognatha* (Santos et al., 2010). LyeTxI shows strong antibacterial and antifungal activities, as well as a weak hemolytic activity in high concentrations. Moreover, this peptide inhibits periodontal pathogens and epithelial cells proliferation

(Consuegra et al., 2013). Recently, our group showed that LyeTxI and its formulation in beta-cyclodextrin, besides being active against periodontopathic bacteria, can also be used to prevent biofilm development (Cruz Olivo et al., 2017).

Nowadays, several efforts have been made to design molecules derived from AMPs with better efficacy, low possibility to induce resistance and with less potential toxicity. Due to the great biotechnological/pharmaceutical potential of LyeTxI, its structure can be used as a template to develop new antibiotics against planktonic bacteria and fungi. Therefore, in the present work, we describe the structure and the biological activity, both *in vitro* (planktonic bacteria) and *in vivo* (a model of septic arthritis in mice), of LyeTxI-b, a peptide derived from LyeTxI. This peptide contains two structure modifications as acetylated N-terminal and a deletion of a His residue. These modifications have altered its structure and improved its activity *in vitro* and *in vivo*.

MATERIALS AND METHODS

Peptide Synthesis and Purification

The peptide LyeTxI-b (CH₃CO-IWLTALKFLGKNLGKLAQQLAKL-NH₂), was synthesized by stepwise solid-phase using the *N*-9-fluorenylmethyloxycarbonyl (Fmoc) strategy (Chan and White, 2000) on a Rink-amide resin (0.68 mmol·g⁻¹). The following side-chain protecting groups were used: *t*-butyl for threonine, *t*-butyloxycarbonyl for lysine and tryptophan, (triphenyl)methyl for asparagine and glutamine. The couplings were performed with 1,3-diisopropylcarbodiimide (DIC), dichloromethane in DMF for 3–4 h. Fmoc deprotection steps were carried out with piperidine/DMF (1:4; v:v) (20 min, twice). The last residue was deprotected and washed to perform the acetylation with a solution comprising 2 mL DMF, 1 mL DCM, 0.11 mol·L⁻¹ DIC and 364.4 μl of 99% acetic anhydride (Sigma-Aldrich) for 40 min. The cleavage step and the side chains deprotection were performed with TFA/thioanisole/water/1,2-ethanedithiol/triisopropylsilane, (86.5/5.0/5.0/2.5/1.0, by volume) at room temperature during 3 h. The final product was precipitated with cold diisopropyl ether and lyophilized.

Two steps RP-HPLC were performed to purify the crude peptide. The first purification was done using a semi-preparative Discovery® BIO Wide Pore C18 column (Supelco), previously equilibrated with 0.1% aqueous TFA (solvent A). The elution was performed with a stepped gradient of acetonitrile in 0.1% TFA (solvent B) (0–40% of solvent B in 4 min; 40–55% of solvent B in 50 min; 55–100% of solvent B in 5 min). The flow was 5.0 mL·min⁻¹ and detection at 220 nm. The PepMap C18™ column (4.6 mm × 150 mm) previously equilibrated with solvent A was used in the second purification. The peptide fraction was eluted with a linear gradient of solvent B (0–100% of solvent B in 30 min). The flow was 1.0 mL·min⁻¹ and detection at 214 nm.

Mass Spectrometry Analysis

The quality of peptide synthesis and purification were evaluated by MALDI-TOF/TOF mass spectrometry analyses carried out on an AutoFlex III instrument (Bruker Daltonics, Billerica, MA,

United States). The samples were co-crystallized with CHCA matrix (1:1, v/v) on MTP AnchorChip 400/384 or 600/384 plates (Bruker Daltonics, Billerica, MA, United States). The instrument was operated in positive reflector mode and the results were analyzed on FlexAnalysis 3.1 (Bruker Daltonics, Billerica, MA, United States).

Circular Dichroism Spectroscopy

The secondary structure preferences of LyeTxI-b were investigated by CD spectroscopy for the peptide in TFE:H₂O solutions (0:100; 10:90; 20:80; 30:70; 40:60; 50:50; 60:40), in the presence of SDS micelles (detergent concentrations ranging from 0.2 to 30.0 mM), and in the presence POPC:POPG (3:1 mol:mol) phospholipid vesicles (lipid concentrations ranging from 0.05 to 2.0 mM). The spectra were recorded at 20°C on a Jasco J-735 spectropolarimeter coupled to a Peltier Jasco PTC-423L (Tokyo, Japan). A rectangular quartz cuvette (1.0 mm path length; NSG, Farmingdale NY, United States) was used. Spectra were acquired from 260 to 190 nm using a 1.0 nm spectral bandwidth, 0.2 nm step resolution, 50 nm.min⁻¹ scan speed, and 1 s response time. 6, 6, and 8 accumulations were, respectively, performed for the peptide samples prepared in TFE:H₂O solutions, in the presence of detergent micelles and in the presence of phospholipid vesicles. Similar experiments with the respective blank solutions were also carried out for background subtraction. The peptide concentration, as determined from the tryptophan molar absorptivity ($\epsilon = 5,550 \text{ M}^{-1} \text{ cm}^{-1}$ at 280 nm), was at 36.5 nmol.L⁻¹ in all CD studies. The POPC:POPG (3:1) phospholipid vesicles were prepared as described elsewhere (Gusmao et al., 2017).

Two-Dimensional Solution NMR Spectroscopy

Two-dimensional solution NMR experiments were carried out to determine the three-dimensional structure of LyeTxI-b. Samples were prepared by dissolving the peptide in a mixture of TFE-*d*₂/H₂O (60:40%, v/v) at 2.0 mM, and the pH was adjusted to 7.0 with 20 mM aqueous phosphate buffer. All NMR experiments were performed at 20°C on a Bruker Avance III spectrometer operating at a ¹H frequency 600.043 MHz. A 5 mm triple-resonance (¹H/¹³C/¹⁵N) gradient probe was used for all experiments. Water suppression was achieved by using pre-saturation. All NMR spectra were processed using NMRPipe (Delaglio et al., 1995).

Total correlation spectroscopy spectrum was acquired using the MLEV-17 pulse sequence (Bax and Davis, 1985) with a spin-lock time of 60 ms. The following parameters were used: spectral width of 6602 Hz, 512 *t*₁ increments were collected with eight transients of 4096 points. NOESY spectra (Kumar et al., 1980) was acquired using mixing times of 80, 100, and 150 ms to check for spin diffusion. The parameters were used as follows: spectral width of 6602 Hz, 512 *t*₁ increments were collected with 32 transients of 4096. ¹H-¹³C HSQC spectra were acquired with F1 and F2 spectral widths of 12820 Hz and 6602 Hz, respectively. 256 *t*₁ increments were collected with 64 transients of 1024 points. Experiments were acquired in an edited mode

in such a way that CH and CH₃ correlations showed a positive phase and CH₂ correlations showed a negative phase (Willker et al., 1993). ¹H-¹⁵N HMQC spectra were acquired with F1 and F2 spectral widths of 1824 Hz and 6602 Hz, respectively, using a fast pulse sequence (Schanda and Brutscher, 2005). 128 *t*₁ increments were collected with 800 transients of 1024 points.

NOE Data and Structure Calculations

The NMR spectra were analyzed using NMRView, version 5.0.3 (Johnson and Blevins, 1994). NOE intensities obtained at 150 ms mixing time were converted into 323 semi-quantitative distance restraints (190 intraresidue, 69 sequential and 64 medium range distance restraints) using the calibration described by Hyberts et al. (1992). The upper limits of the distance restraint thus obtained were 2.8, 3.4, and 5.0 Å (strong, medium, and weak NOE, respectively). Forty-four dihedral angle restraints were obtained from analysis of C α , H α , C β , N, and HN chemical shifts with the program TALOS+ (Shen et al., 2009). Structure calculations were performed using the Xplor-NIH software, version 2.27 (Schwieters et al., 2003). A total of 100 structures, starting with an extended conformation, were generated using a simulated annealing protocol, followed by 20,000 steps of simulated annealing at 1,000 K and a subsequent decrease in temperature in 15,000 steps in the first slow-cool annealing stage. The stereochemical quality of the lowest energy structures was analyzed by PROCHECK-NMR (Laskowski et al., 1996). The display, analysis, and manipulation of the three-dimensional structures were performed with the program MOLMOL (Koradi et al., 1996).

Antimicrobial Tests

Strains of *Escherichia coli* (ATCC 25922) and *Staphylococcus aureus* (ATCC 25923) were cultured on BHI agar in aerobic conditions, while strains of *Aggregatibacter actinomycetemcomitans* (ATCC 29522) and *Streptococcus sanguinis* (ATCC 10556) were cultured on BHI in anaerobic conditions. The MIC using the microdilution method was performed to determine the bacterial susceptibility to AMPs, as previously described (Wiegand et al., 2008). Samples of LyeTxI-b were serially diluted from 91.25 to 0.17 $\mu\text{mol/L}$ in MH broth and incubated with 10⁵ CFU/well for 24 h at 37°C. MIC was defined as the lowest concentration of the peptide that prevented the visible growth of the microorganism. Also, minimum bactericidal concentrations (MBCs) values were determined by plating an aliquot of MIC values by well, with no visible turbidity, in BHI agar, in aerobic conditions for *E. coli* and *S. aureus*, and in anaerobic conditions for *A. actinomycetemcomitans* and *S. sanguinis*. After 24–48 h of growth, the MBC value was determined as the lowest concentration of peptide with no visible bacterial growth on the surface of the agar. MIC and MBC assays were performed in triplicate.

Hemolytic Assay

The hemolytic assays were performed as previously described (Santos et al., 2010), with modifications. Briefly, lamb

erythrocytes were incubated with a serial concentration dilution of the peptide ($91.25 \mu\text{mol.L}^{-1}$ to $0.17 \mu\text{mol.L}^{-1}$) for 1 h at 37°C . The released hemoglobin was measured using a spectrophotometry at 405 nm. Triton X-100% was used as positive control.

Experimental Models of Arthritis

Staphylococcus aureus-Induced Arthritis

Staphylococcus aureus ATCC 6538 was grown in BHI agar supplement with 5% of sheep blood for 24 h. The inoculum (10^7CFU.mL^{-1}) was injected into the tibiofemoral joint of anesthetized C57BL/6j mice as described (Amaral et al., 2016), while negative controls received saline injections. Treatments were performed directly into the joint, with LyeTxI-b (0.03 nmol), clindamycin (7.0 nmol) or saline, each starting 48 h after the bacterial injection. Seven days after the injection of the inoculum, mice were euthanized under an overdose of ketamine/xylazine anesthesia, followed by cervical dislocation, for analyses.

Antigen-Induced Arthritis (AIA)

C57BL/6j mice were immunized on day 1 with intradermal injection of 500 μg of mBSA (Sigma-Aldrich, St Louis, MO, United States) in 50 μL PBS emulsified in 50 μL Freund's complete adjuvant (CFA; Sigma-Aldrich). Fourteen days later, the antigen challenge was performed by injecting 10 μg mBSA (in 10 μL sterile saline) in the right knee joint of each mouse. Mice were then intra-articularly treated with LyeTxI-b (0.03 nmol) 1 h before the challenge and 3 h after the challenge. All procedures were performed under ketamine/xylazine anesthesia, and all efforts were made to minimize animal suffering. Analyses were conducted 24 h after the challenge. Non-immunized mice were used as negative controls. Euthanasia was performed as mentioned above.

In vivo experiments were carried out in accordance and approved by the local Animal Experiment Ethics Committee (CETEA-UFMG; protocol no. 236/2014).

Inflammatory Parameters Analysis

After mice euthanasia, the intra-articular cavity was exposed and washed with PBS containing 3% of bovine serum albumin ($2 \times 5 \mu\text{L}$). The total number of leukocytes and differential leukocytes was counted using a Neubauer chamber and cytopsin preparations (Shandon III; Thermo Shandon, Frankfurt, Germany) stained with May–Grunwald–Giemsa, respectively. Then, the periarticular tissue was removed for cytokine analyses. IL-1 β and CXCL1 chemokine concentrations were measured using a commercially available enzyme-linked immunosorbent assay (ELISA), following the instructions supplied by the manufacturer (R&D Systems, Minneapolis, MN, United States).

In another set of experiments, mice were euthanized for the analysis of proteoglycan loss in joint cartilage, a marker of cartilage damage. Tissue was fixed in 10% buffered formalin (pH 7.4), decalcified for 30 days in 14% EDTA. Samples were embedded in paraffin and then sectioned and stained with toluidine blue. Two sections/knee joint were microscopically

examined by a single pathologist to estimate joint proteoglycan content, as previously described (Urech et al., 2010). The joint surface images of each sample were acquired and analyzed using ImageJ software (National Institutes of Health, Bethesda, MD, United States). Cartilage proteoglycan content was defined as the percentage of TB-stained area in relation to the total evaluated cartilage surface.

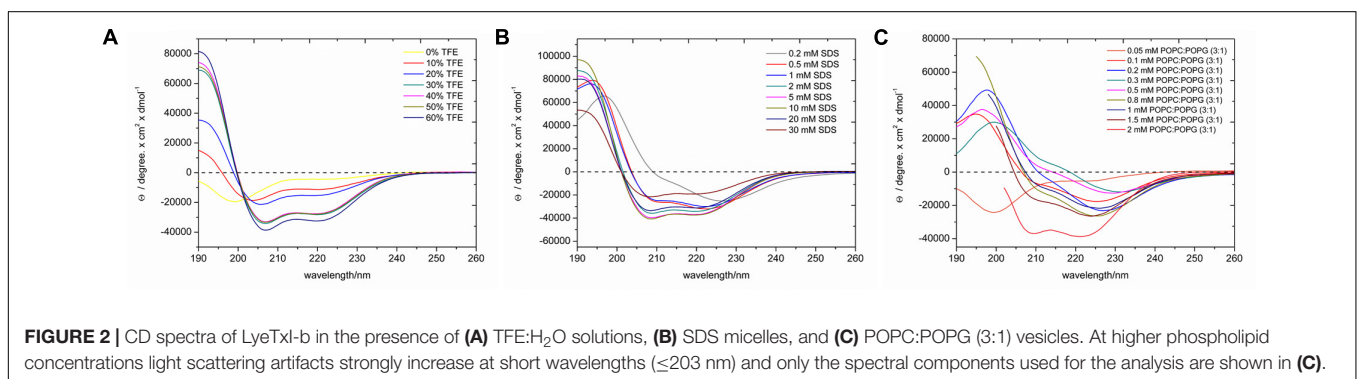
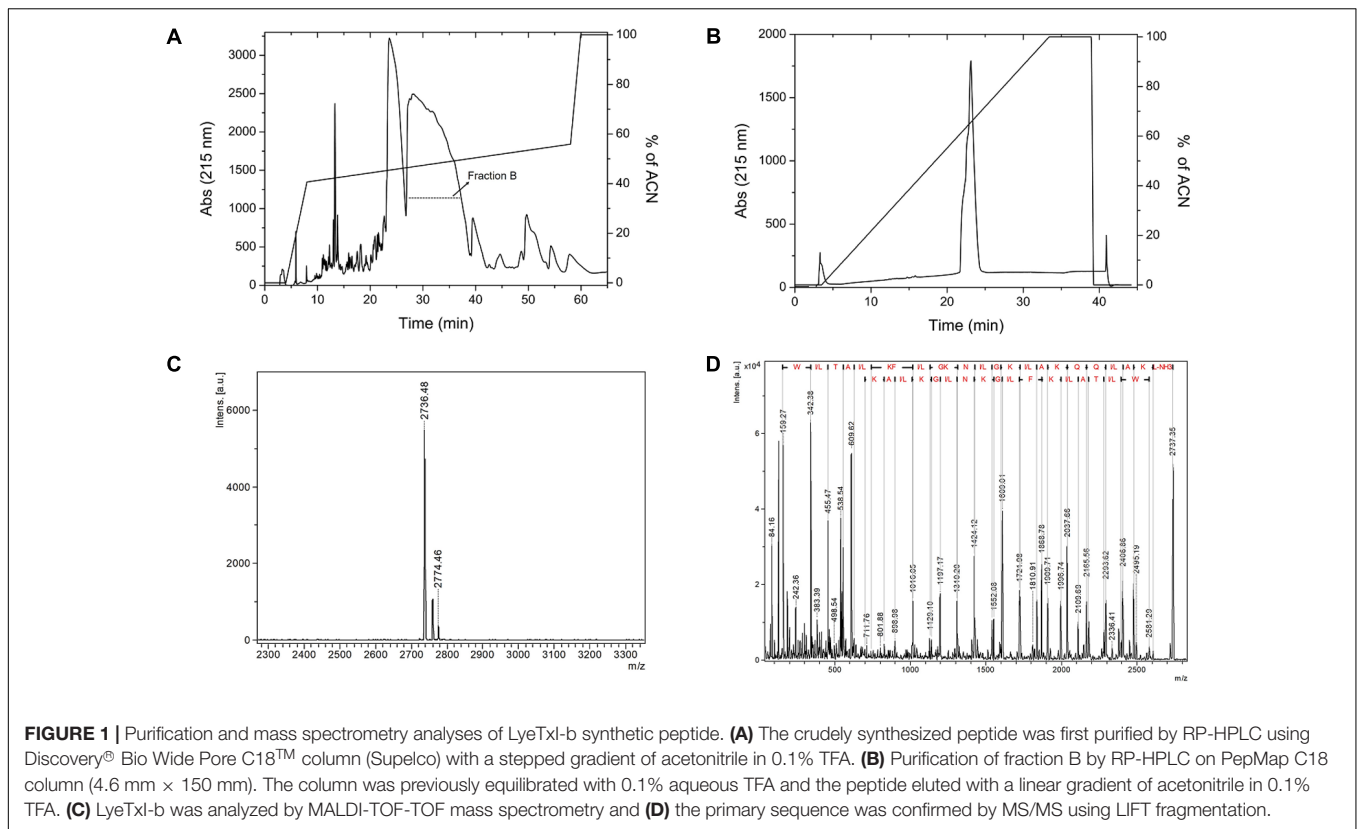
RESULTS AND DISCUSSION

Synthesis and Liquid Chromatography

After chemical synthesis, we purified the peptide using two-step RP-HPLC. The first RP-HPLC assay on Discovery® BIO Wide Pore C18 column (Figure 1A) shows two major fractions eluted with an acetonitrile gradient (50–55% of solvent), named fraction A and fraction B. Only fraction B was submitted to another RP-HPLC experiment on a PepMap C18™ (Figure 1B), and the relative purity of the fraction was analyzed by MALDI-TOF/TOF mass spectrometry. The peptide of interest was eluted in fraction B, which was evidenced by a higher *m/z* intensity 2736.4, corresponding to the expected mass of the N-terminally acetylated peptide (MW 2737.3 Da) (Figure 1C). The peptide was therefore named LyeTxI-b. To confirm the primary structure of LyeTxI-b, this compound was subjected to MS/MS fragmentation (Figure 1D).

Circular Dichroism Spectroscopy

LyeTxI-b exhibits random coil conformations in the aqueous environment, as evidenced by the minimum near 200 nm in Figure 2A. Upon addition of TFE, the peptide adopts a helical conformation, as noticed by the appearance of two minima near 208 and 222 nm and a maximum near 192 nm (Figure 2A), which show relatively small intensities up to 20% of TFE, however, significant increases are observed in solutions containing 30–50% of TFE, which present very similar spectral profiles. This is a very common feature of linear cationic AMPs peptides, which show no conformational preferences in aqueous environments, whereas well-defined conformations are observed in the presence of organic co-solvents or other membrane mimetic environments (Gusmao et al., 2017). Interestingly the spectrum obtained for the peptide in the presence of 60% of TFE is consistent with even higher helical contents. Some investigations using small angle X-ray and dynamic light scattering of different alcohol–water solutions have indicated the formation local clusters, which reach maximum size at about 40% of the co-solvent in the case of TFE:H₂O mixtures, whereas higher concentrations of TFE lead to smaller size clusters due to a higher homogeneity of the respective solutions (Kuprin et al., 1995; Gast et al., 2001; Othon et al., 2009). The larger aggregates may reduce the local polarity near the peptide and induce intramolecular bond formation or peptide aggregation, which can be correlated to differences in helicity. Since a higher helicity is observed in the presence of 60% of TFE and to avoid complications due to the formation of local aggregates, we decided to investigate in atomic detail the three-dimensional structure of LyeTxI-b by



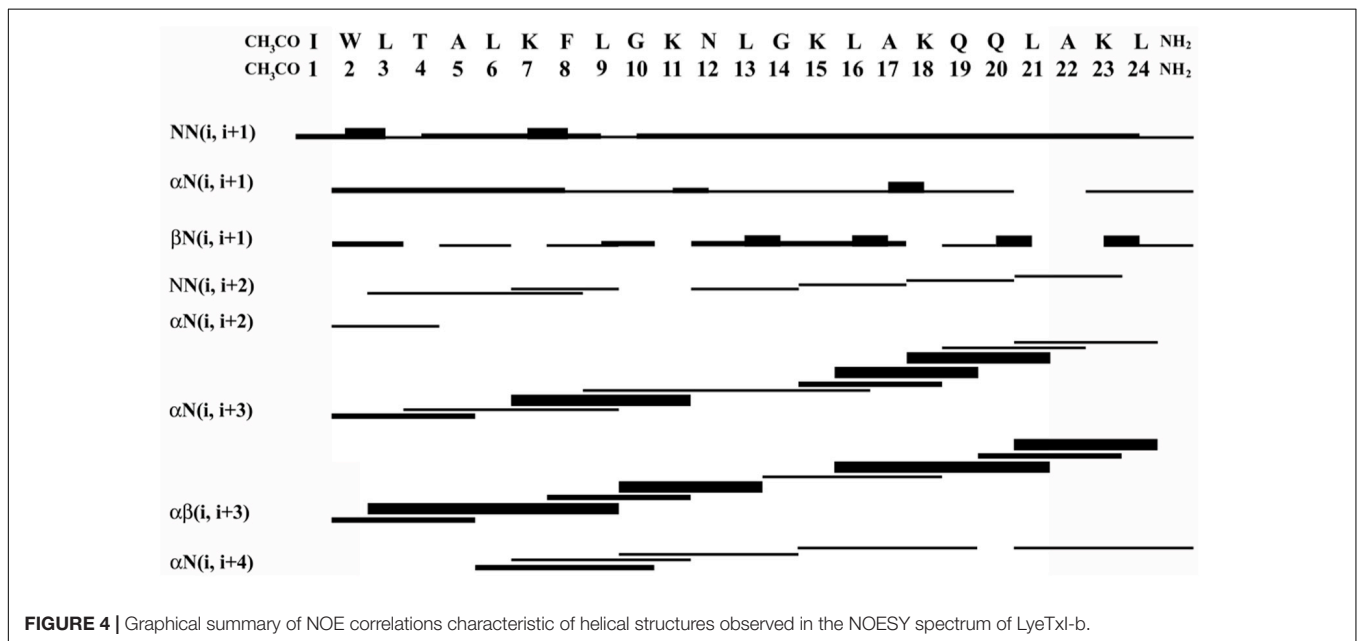
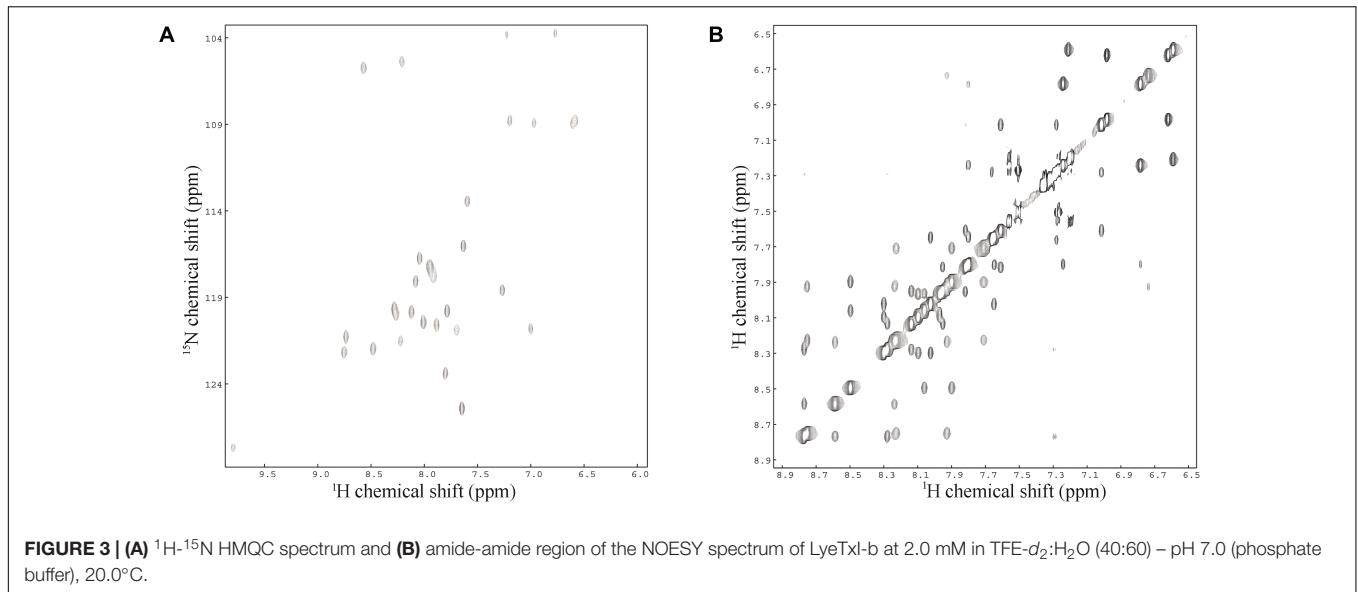
NMR spectroscopy in a solution containing 60% of the co-solvent (see below).

In order to confirm the helical conformation in membrane mimetic environments, the secondary structural preferences were also investigated in the presence of SDS micelles and POPC:POPG (3:1) vesicles and spectra with helical profiles were observed in both cases. In the presence of the micellar detergent (**Figure 2B**), the intensities of the characteristic maximum and minima increase with the SDS concentration until a plateau (5 mM of SDS) is reached. In the presence of vesicles (**Figure 2C**), the minimum and maxima intensities also increase with the phospholipid concentration, however, significant augments in the two minima intensities are observed at 2 mM of phospholipids. These results indicate that the peptide adopts well-defined helical conformations in the presence of phospholipid vesicles, however,

a membrane-bound (helical) and a water-soluble (random coil) states coexist at smaller phospholipid to peptide ratios, as previously observed for other AMPs (Voievoda et al., 2015).

Two-Dimensional Solution NMR Spectroscopy

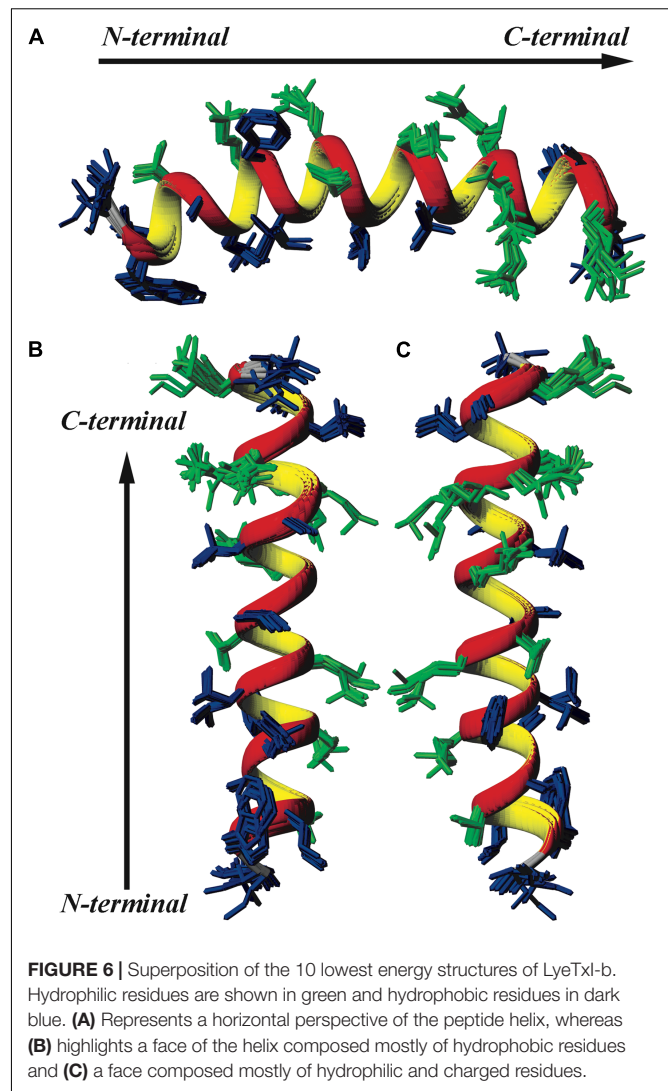
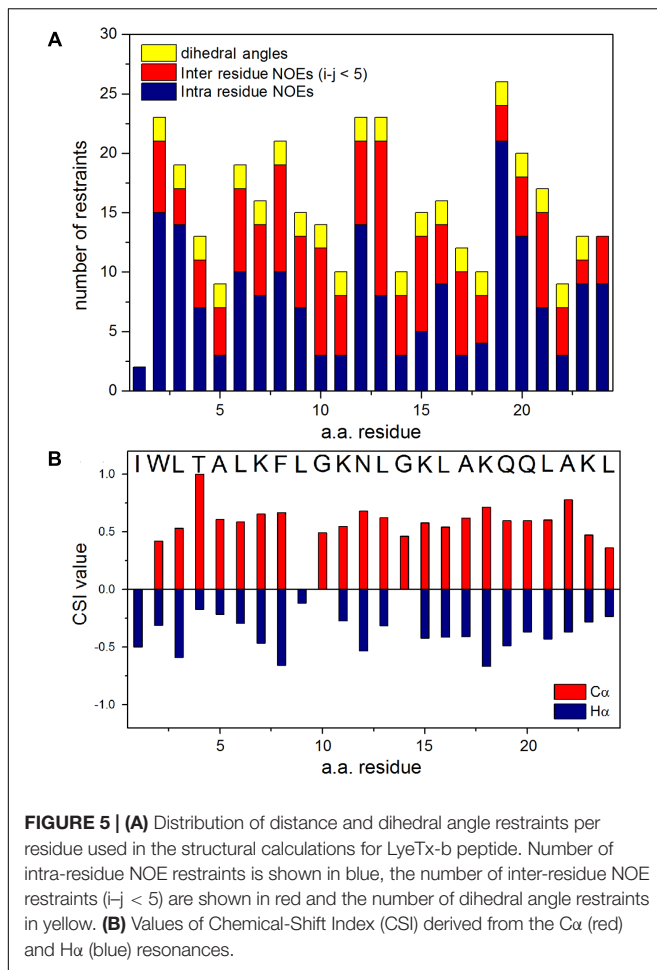
Sequence-specific assignments have been performed from simultaneous analysis of NMR contour maps, as previously indicated (Resende et al., 2008). The dispersion of chemical shifts observed in the ¹H-¹⁵N HMQC spectrum, as well as the high number of cross-peaks detected in the NOESY contour map (**Figure 3**) indicate a well-folded peptide conformation. **Figure 4** presents the summary of through-space correlations that characterize peptide secondary structure, obtained from NOESY. In accordance with the data obtained from CD



spectroscopy at similar conditions, several NN ($i, i+1$), αN ($i, i+3$), $\alpha\beta$ ($i, i+3$) and αN ($i, i+4$) connections indicate that the peptide presents a well-defined helical segment from Trp-2 to the last amino acid residue, including the C-terminal carboxamide, which is involved in an αN ($i, i+4$) interaction. The distribution of distance and dihedral angle restraints per residue are presented in **Figure 5A**. This trend of α -helix secondary structure is also confirmed by the $\text{H}\alpha$ and $\text{C}\alpha$ chemical shift indexes (CSI) (Wishart et al., 1992; Tremblay et al., 2010), as presented in the **Figure 5B**. **Figure 6** presents the overlap of the 10 most stable structures obtained after simulated annealing protocol. This set of structures showed RMSD values of 0.98 and 0.46 Å for the superposition of all heavy and of the backbone atoms, respectively, and all of the ϕ and ψ angular pairs are located in

the most favorable regions of the Ramachandran Plot (data from PROCHECK NMR), indicating the good quality of the structural model obtained.

Similarly to LyeTxI (Santos et al., 2010), LyeTxI-b α -helix does not show a clear partition between hydrophobic and hydrophilic faces, which is observed for many other antibiotic peptides, such as phylloseptins and dermadistinctin K (Resende et al., 2008; Verly et al., 2009). However, LyeTxI-b presents a higher structural stability near the N-terminus when compared to the native peptide LyeTxI, since LyeTxI-b helix is defined by a greater number of medium-range NOEs near the N-terminus, especially medium and strong-intensity $\alpha\beta$ ($i, i+3$) correlations. The higher structural stability near LyeTxI-b N-terminus is certainly related to the terminal amine acetylation, which eliminates the



positive charge and stabilizes the positive end of the helix dipole. The acetylation also allows extra hydrogen bond interactions involving the acetyl carbonyl group and the amidic hydrogens near N-terminus. Extra hydrogen bonds interactions, as well as helix dipole neutralization properties due to either C-terminal carboxamidation or N-terminus acetylation, are known to promote structural stability in helical segments (Resende et al., 2008; Zanin et al., 2016). An interesting feature observed for the LyeTxI-b structure is a helix curvature (Figure 3A), which is correlated to the NN ($i, i+2$) NOE correlations involving several residues of the helical segment. This sort of NOEs was observed for the native peptide with a minor proportion, inducing a less pronounced curvature of the peptide helix (Santos et al., 2010).

Another example of an AMP that does not show an amphipathic partition is the Htr-M, in which a lysine residue represents a discontinuity within the helix hydrophobic face. This discontinuity has an important structural role in the homodimeric peptide homotarsinin (Htr), since the positively charged side chain of this lysine residue interacts with a negatively charged aspartate residue and a hydrophilic serine residue of the other peptide chain. These electrostatic interactions are important to stabilize the homodimer coiled coil three-dimensional structure (Verly et al., 2017).

Antimicrobial Activity in Planktonic Culture

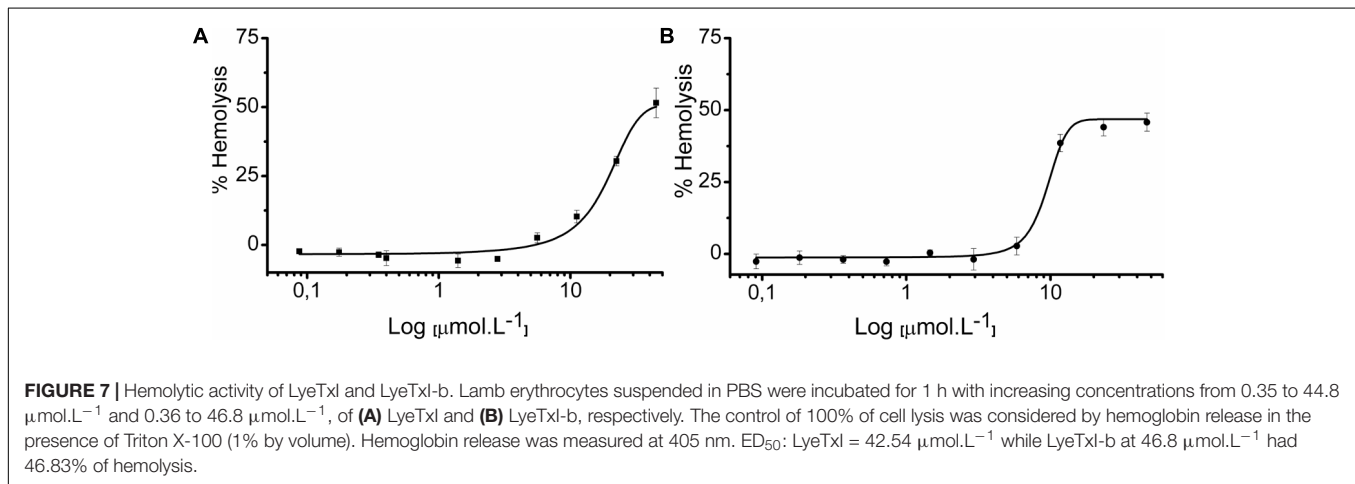
LyeTxI-b showed a potent antimicrobial inhibition activity against Gram-positive and Gram-negative planktonic bacteria under aerobic and anaerobic conditions (Table 1). We observed that LyeTxI-b was exceptionally active against *E. coli* and *S. aureus*. The MBC values were the same as those obtained for MIC in all tests. The topic antibiotic chlorhexidine acetate was used as a positive control.

The MIC value of LyeTxI-b for *E. coli* was 10-fold higher when compared to that of the LyeTxI peptide (Santos et al., 2010). On the other hand, the activity of LyeTxI-b for *S. aureus* was similar to the previously observed for the native peptide (Santos et al., 2010). Moreover, LyeTxI-b was able to decreased around 50% of MBC but with similar MIC in *A. actinomycetemcomitans*, when compared to the original peptide in the work of Consuegra et al. (2013). It is known that the lipid composition of the plasma membrane considerably affects the action of AMPs (to review Malanovic and Lohner, 2016; Malmsten, 2016). Gram-negative

TABLE 1 | Minimum inhibitory concentration (MIC) and minimum bactericidal concentration (MBC) of LyeTxI-b and chlorhexidine acetate.

Compound	<i>E. coli</i>		<i>S. aureus</i>		<i>A. actinomycetemcomitans</i>		<i>S. sanguinis</i>	
	MIC $\mu\text{mol.L}^{-1}$	MBC $\mu\text{mol.L}^{-1}$	MIC $\mu\text{mol.L}^{-1}$	MBC $\mu\text{mol.L}^{-1}$	MIC $\mu\text{mol.L}^{-1}$	MBC $\mu\text{mol.L}^{-1}$	MIC $\mu\text{mol.L}^{-1}$	MBC $\mu\text{mol.L}^{-1}$
LyeTxI	7.81**	–	–	–	10.6*	20.12*	10.9***	21.8***
LyeTxI-b	0.71	0.71	2.85	2.85	11.4	11.4	5.7	5.7
Chlorhexidine acetate	125	–	31	–	125	–	62.5	–

Data of LyeTxI were obtained from (Consuegra et al., 2013) *; (Santos et al., 2010) **; (Cruz Olivo et al., 2017) *** and correspond to the same strain references used to LyeTxI-b.



bacteria, in their majority, present a higher concentration of the zwitterionic lipid phosphatidylethanolamine when compared with Gram-positive bacteria (Epanand and Epanand, 2011).

In general, LyeTxI-b has antimicrobial activity at μmol concentrations, similarly to previously described AMPs, such as magainins, LL-37 and others (Park et al., 2009; Joshi et al., 2010; Brogden and Brogden, 2011; Haisma et al., 2014; Ageitos et al., 2017).

Hemolytic Assays

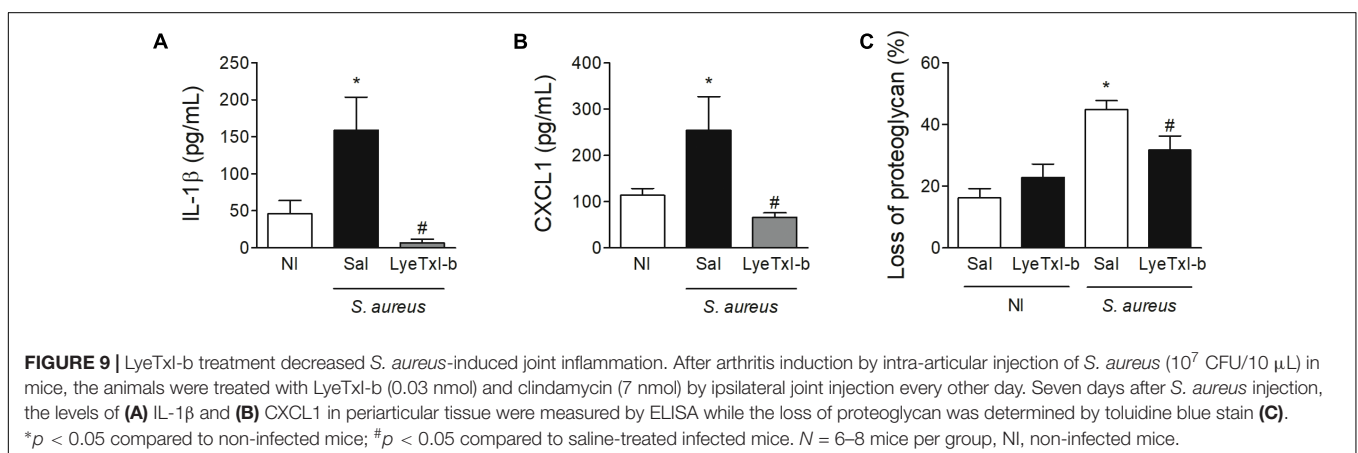
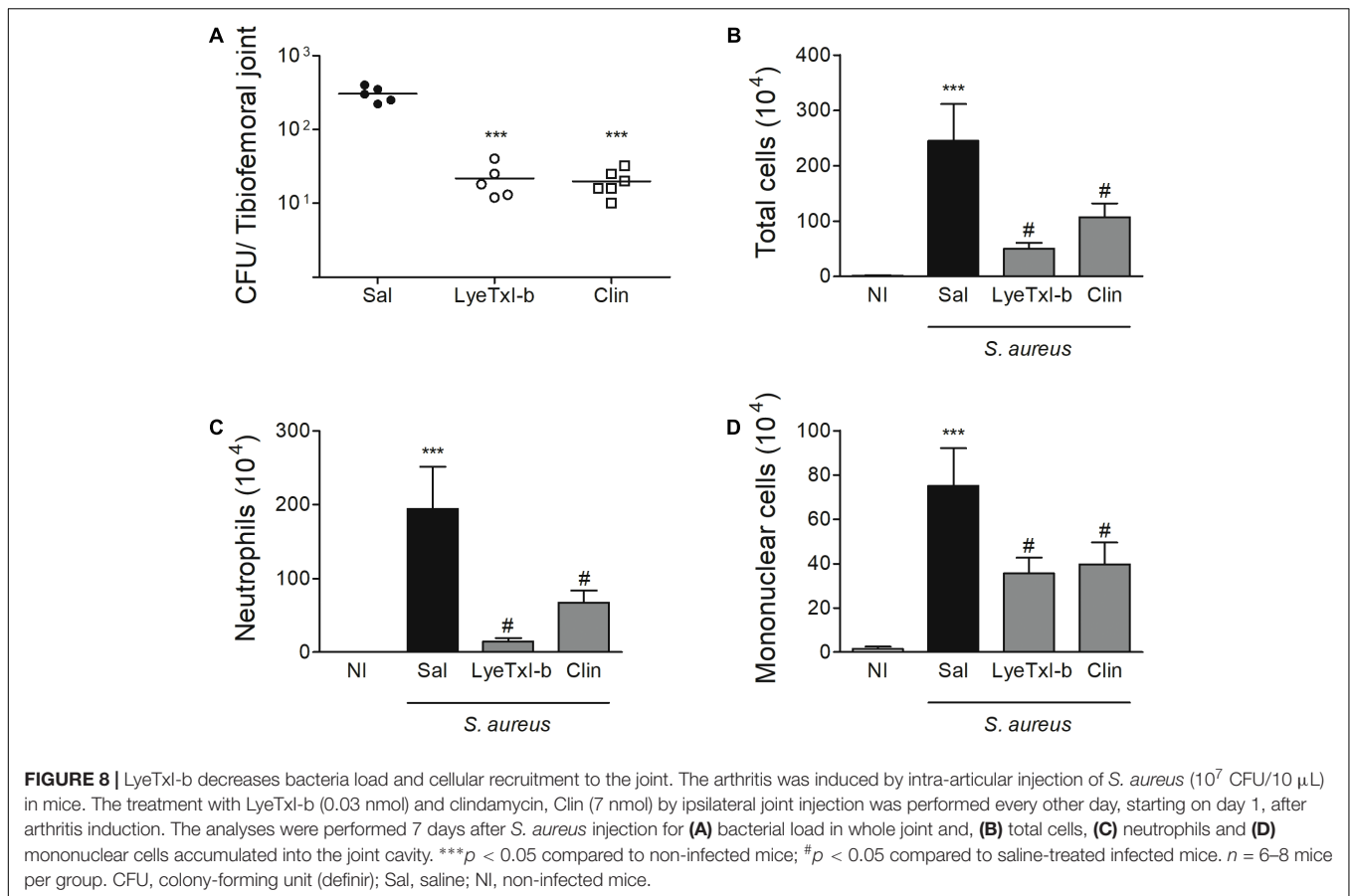
Our group previously demonstrated the hemolytic capacity of LyeTxI, with an ED_{50} of 130 μM on rabbit erythrocytes (Santos et al., 2010). Therefore, we also tested the hemolytic activity of LyeTxI-b, to evaluate if the loss of an amino acid residue and the N-terminus acetylation would modify this property. In this work, we performed the assay on lamb erythrocytes, for both peptides. As shown in **Figure 7**, LyeTxI had an ED_{50} value of 42.54 $\mu\text{mol.L}^{-1}$, while LyeTxI-b showed approximately 46.83% of hemolysis at 46.6 $\mu\text{mol.L}^{-1}$. This result indicates a slight increase in LyeTxI-b activity on eukaryotic cells, which is not significant, considering its 10-fold increase in bactericidal capacity for *E. coli*. Moreover, we observed a high level of hemolysis for LyeTxI in lamb erythrocytes, when compared to rabbits. It is known that mammalian species differ in their erythrocyte susceptibility, and lamb erythrocytes have been considered more fragile than those from rabbit (Matsuzawa and Ikarashi, 1979). In addition, it may be pointed out that in recent results obtained by our group (not shown) LyeTxI-b showed only mild cytotoxicity against

lung and kidney normal cell lines (Abdel-Salam et al., work in submission).

LyeTxI-b Controls Bacterial Growth and Tissue Inflammation *in Vivo*

Considering our positive results regarding LyeTxI-b activity in the MIC assay, we evaluated the effectiveness of this peptide in a model of *S. aureus*-induced arthritis in mice (Boff et al., 2018). Initially, we determined the MIC for *S. aureus* ATCC 6538, since the strain used in this model was different from the previous MIC assay. The MIC value for LyeTxI-b was 2.85 $\mu\text{mol.L}^{-1}$, while for clindamycin it was 367 $\mu\text{mol.L}^{-1}$ (control). It is noteworthy that in the growth inhibition tests we used 10^5 CFU.mL⁻¹ while the SA model was established with 10^7 CFU.mL⁻¹. Therefore, the MIC concentrations used was two-fold higher for the *in vivo* test. Thus, for each 10 μL injection in treatment models, 80 ng of LyeTxI-b and 3120 μg of clindamycin were applied.

Staphylococcus aureus-induced joint inflammation is associated with a massive recruitment of neutrophils to the joint that, together with the presence of bacteria, cause articular damage and pain (Mathews et al., 2010). In this model, a high concentration of bacteria can be detected in the joint 7 days after the challenge, and the treatment with LyeTxI-b reduced this number (**Figure 8A**). Furthermore, LyeTxI-b reduces cell accumulation in *S. aureus*-challenged joint, including the number of total cells, neutrophils and mononuclear cells (**Figures 8B–D**). Therefore, we can speculate that both treatments, using LyeTxI-b and clindamycin, were able to decrease the pain symptom,



since the pain process can be associated with the mediators released by neutrophils (Sachs et al., 2011), as well as the direct activation of nociceptors by *S. aureus* (Chiu et al., 2013). It is worth mentioning that the treatment with the peptide decreased the bacterial load to the same level as the antibiotic treatment, not showing significant difference between the groups in the experimental model of SA. However, the therapeutic concentration of our peptide was more than two hundred lower (0.03 nmol) compared to that of the antibiotic (7 nmol), indicating its higher potency.

Similarly, the treatment with LyeTxI-b and clindamycin also reduced the level of IL-1 β pro-inflammatory cytokine and CXCL1 chemokine in the joint, when compared to non-treated joints (Figures 9A,B). IL-1 β has been shown as an important factor in the pathogenesis of septic arthritis in an experimental model of intravenous injection (Hultgren et al., 2002) and CXCL1 is essential for the recruitment of neutrophils (Lira et al., 1994). Another important characteristic of septic arthritis is tissue damage. Here, the injection of *S. aureus* caused an important loss of proteoglycans on articular cartilages while the treatment

with LyeTxI-b preserved the integrity of the joint (Figure 9C). Importantly, the injection of LyeTxI-b in naïve joint did not cause tissue inflammation.

Our results show that LyeTxI-b-treated mice present decreased bacteria load and inflammation in the joint similar to clindamycin but in different concentration, as mentioned above. Since the presence of bacteria in a joint is sufficient to stimulate resident cells to produce pro-inflammatory mediators and cell recruitment, the reduced number of bacteria in LyeTxI-b-treated group could be enough to reduce all other inflammatory markers, as observed in Figures 8, 9. Thus, we questioned whether LyeTxI-b could have a direct role in the reduction of joint inflammation, independently on its bactericidal/bacteriostatic property. To answer this question, we used an experimental model of immunization-induced arthritis (without infection – AIA model). The treatment with LyeTxI-b did not alter the recruitment of neutrophils to the joint, which are important markers of tissue inflammation in this model (AIA: $146.08 \pm 15.87 - n = 5$, AIA + LyeTxI_b: $162.28 \pm 12.71 - n = 6$; mean \pm SEM). Thus, this result showed a non-direct role of LyeTxI-b on joint inflammation, and the reduction of *S. aureus*-induced arthritis seems to be caused by the control of bacterial growth in the joint. In sum, the ability of LyeTxI-b to control bacterial growth in the joint is sufficient to reduce the main inflammatory markers of SA model. In addition, preliminary nociceptive assays using an electronic version of von Frey test with LyeTxI-b in mice did not show any effect (data not shown).

Since the treatment of SA patients mostly involves use of antibiotics and considering that an increased number of patients infected with bacteria are resistant to antibiotics, the development of new therapeutic options became essential for a better control of infection and tissue damage (Weston et al., 1999; Sharff et al., 2013). Thus, LyeTxI-b is a prominent model for the development of new antibiotics.

REFERENCES

- Ageitos, J. M., Sánchez-Pérez, A., Calo-Mata, P., and Villa, T. G. (2017). Antimicrobial peptides (AMPs): ancient compounds that represent novel weapons in the fight against bacteria. *Biochem. Pharmacol.* 133, 117–138. doi: 10.1016/j.bcp.2016.09.018
- Amaral, F. A., Boff, D., and Teixeira, M. M. (2016). *In Vivo* models to study chemokine biology. *Methods Enzymol.* 570, 261–280. doi: 10.1016/bs.mie.2015.09.015
- Andersson, D. I., Hughes, D., and Kubicek-Sutherland, J. Z. (2016). Mechanisms and consequences of bacterial resistance to antimicrobial peptides. *Drug Resist. Updat.* 26, 43–57. doi: 10.1016/j.drup.2016.04.002
- Azim, S., McDowell, D., Cartagena, A., Rodriguez, R., Laughlin, T. F., and Ahmad, Z. (2016). Venom peptides cathelicidin and lycotoxin cause strong inhibition of *Escherichia coli* ATP synthase. *Int. J. Biol. Macromol.* 87, 246–251. doi: 10.1016/j.ijbiomac.2016.02.061
- Bax, A., and Davis, D. G. (1985). MLEV-17-based two-dimensional homonuclear magnetization transfer spectroscopy. *J. Magn. Reson.* 65, 355–360. doi: 10.1016/0022-2364(85)90018-6
- Bechinger, B., and Gorr, S. U. (2017). Antimicrobial peptides: mechanisms of action and resistance. *J. Dent. Res.* 96, 254–260. doi: 10.1177/0022034516679973
- Boff, D., Oliveira, V. L. S., Queiroz Junior, C. M., Silva, T. A., Allegretti, M., Verri, W. A. Jr., et al. (2018). CXCR2 is critical for bacterial control and

CONCLUSION

In the present work, we characterized LyeTxI-b, a peptide derived from the spider toxin LyeTxI, with two modifications: removal of a single amino acid residue and N-terminus acetylation. We show that these small alterations are able to improve the antibiotic activity of the peptide. This is also observed in the organisms under study, i.e., different strains of the same microorganism or different species may have different susceptibilities to the drug. Therefore, our results contribute to the emerging area of antibiotics derived from AMPs, as a new alternative for the treatment of infections that are resistant to conventional drugs.

AUTHOR CONTRIBUTIONS

PR synthesized and purified the peptide and performed MALDI-TOF and CD analyses. RV and JR performed the NMR experiments and analyzed the CD and NMR data. PR and MC investigated the study on MIC. PR and MM-B investigated the study on hemolysis. DB and FA investigated the study on *in vivo* model. PR and MdL wrote the original draft. PR, MM-B, MC, AP, FA, JR, and MdL wrote, reviewed, and edited the manuscript. MdL envisioned the concept. DS, AP, and MdL supervised the study.

FUNDING

This study was supported by Conselho Nacional de Desenvolvimento Científico e Tecnológico (CNPq), Coordenação de Aperfeiçoamento de Pessoal de Nível Superior (CAPES), Fundação de Amparo à Pesquisa do Estado de Minas Gerais (FAPEMIG), and Instituto Nacional de Ciência e Tecnologia em Toxinas (INCTTOX).

- development of joint damage and pain in *Staphylococcus aureus*-induced septic arthritis in mouse. *Eur. J. Immunol.* 48, 454–463. doi: 10.1002/eji.201747198
- Brogden, K. A. (2005). Antimicrobial peptides: pore formers or metabolic inhibitors in bacteria? *Nat. Rev. Microbiol.* 3, 238–250. doi: 10.1038/nrmicro1098
- Brogden, N. K., and Brogden, K. A. (2011). Will new generations of modified antimicrobial peptides improve their potential as pharmaceuticals? *Int. J. Antimicrob. Agents* 38, 217–225. doi: 10.1016/j.ijantimicag.2011.05.004
- Bulet, P., Hetru, C., Dimarcq, J. L., and Hoffmann, D. (1999). Antimicrobial peptides in insects; structure and function. *Dev. Comp. Immunol.* 23, 329–344. doi: 10.1016/S0145-305X(99)00015-4
- Chan, W. C., and White, P. D. (2000). *Fmoc Solid Phase Peptide Synthesis: A Practical Approach*. Oxford: Oxford University Press.
- Chiu, I. M., Heesters, B. A., Ghasemlou, N., Von Hehn, C. A., Zhao, F., Tran, J., et al. (2013). Bacteria activate sensory neurons that modulate pain and inflammation. *Nature* 501, 52–57. doi: 10.1038/nature12479
- Consuegra, J., de Lima, M. E., Santos, D., Sinisterra, R. D., and Cortés, M. E. (2013). Peptides: β -cyclodextrin inclusion compounds as highly effective antimicrobial and anti-epithelial proliferation agents. *J. Periodontol.* 84, 1858–1868. doi: 10.1902/jop.2013.120679
- Cruz Olivo, E. A., Santos, D., de Lima, M. E., Dos Santos, V. L., Sinisterra, R. D., and Cortes, M. E. (2017). Antibacterial effect of synthetic peptide LyeTxI and LyeTxI/beta-Cyclodextrin association compound against planktonic and

- multispecies biofilms of periodontal pathogens. *J. Periodontol.* 88, e88–e96. doi: 10.1902/jop.2016.160438
- Datta, A., Ghosh, A., Airoidi, C., Sperandio, P., Mroue, K. H., Jimenez-Barbero, J., et al. (2015). Antimicrobial peptides: insights into membrane permeabilization, lipopolysaccharide fragmentation and application in plant disease control. *Sci. Rep.* 5:11951. doi: 10.1038/srep11951
- Dawson, R. M., and Liu, C. Q. (2008). Properties and applications of antimicrobial peptides in biodefense against biological warfare threat agents. *Crit. Rev. Microbiol.* 34, 89–107. doi: 10.1080/10408410802143808
- de la Fuente-Nunez, C., Cardoso, M. H., de Souza Candido, E., Franco, O. L., and Hancock, R. E. (2016). Synthetic antibiofilm peptides. *Biochim. Biophys. Acta* 1858, 1061–1069. doi: 10.1016/j.bbame.2015.12.015
- de la Fuente-Nunez, C., Refouveille, F., Fernandez, L., and Hancock, R. E. (2013). Bacterial biofilm development as a multicellular adaptation: antibiotic resistance and new therapeutic strategies. *Curr. Opin. Microbiol.* 16, 580–589. doi: 10.1016/j.mib.2013.06.013
- Delaglio, F., Grzesiek, S., Vuister, G. W., Zhu, G., Pfeifer, J., and Bax, A. (1995). NMRPipe: a multidimensional spectral processing system based on UNIX pipes. *J. Biomol. NMR* 6, 277–293. doi: 10.1007/BF00197809
- Dobson, A. J., Purves, J., Kamysz, W., and Rolff, J. (2013). Comparing selection on *S. aureus* between antimicrobial peptides and common antibiotics. *PLoS One* 8:e76521. doi: 10.1371/journal.pone.0076521
- Epanand, R. M., and Epanand, R. F. (2011). Bacterial membrane lipids in the action of antimicrobial agents. *J. Pept. Sci.* 17, 298–305. doi: 10.1002/psc.1319
- Gast, K., Siemer, A., Zirwer, D., and Damaschun, G. (2001). Fluoroalcohol-induced structural changes of proteins: some aspects of cosolvent-protein interactions. *Eur. Biophys. J.* 30, 273–283. doi: 10.1007/s002490100148
- Ghosh, A., Kar, R. K., Jana, J., Saha, A., Jana, B., Krishnamoorthy, J., et al. (2014). Indolicidin targets duplex DNA: structural and mechanistic insight through a combination of spectroscopy and microscopy. *ChemMedChem* 9, 2052–2058. doi: 10.1002/cmdc.201402215
- Gusmao, K. A. G., Dos Santos, D. M., Santos, V. M., Cortes, M. E., Reis, P. V. M., Santos, V. L., et al. (2017). Ocellatin peptides from the skin secretion of the South American frog *Leptodactylus labyrinthicus* (Leptodactylidae): characterization, antimicrobial activities and membrane interactions. *J. Venom Anim. Toxins Incl. Trop. Dis.* 23:4. doi: 10.1186/s40409-017-0094-y
- Haisma, E. M., de Breijl, A., Chan, H., van Dissel, J. T., Drijfhout, J. W., Hiemstra, P. S., et al. (2014). LL-37-derived peptides eradicate multidrug-resistant *Staphylococcus aureus* from thermally wounded human skin equivalents. *Antimicrob. Agents Chemother.* 58, 4411–4419. doi: 10.1128/AAC.02554-14
- Hultgren, O. H., Svensson, L., and Tarkowski, A. (2002). Critical role of signaling through IL-1 receptor for development of arthritis and sepsis during *Staphylococcus aureus* infection. *J. Immunol.* 168, 5207–5212. doi: 10.4049/jimmunol.168.10.5207
- Hyberts, S. G., Goldberg, M. S., Havel, T. F., and Wagner, G. (1992). The solution structure of eglin c based on measurements of many NOEs and coupling constants and its comparison with X-ray structures. *Protein Sci.* 1, 736–751. doi: 10.1002/pro.5560010606
- Jenssen, H., Hamill, P., and Hancock, R. E. (2006). Peptide antimicrobial agents. *Clin. Microbiol. Rev.* 19, 491–511. doi: 10.1128/CMR.00056-05
- Johnson, B. A., and Blevins, R. A. (1994). NMR View: a computer program for the visualization and analysis of NMR data. *J. Biomol. NMR* 4, 603–614. doi: 10.1007/BF00404272
- Joshi, S., Bisht, G. S., Rawat, D. S., Kumar, A., Kumar, R., Maiti, S., et al. (2010). Interaction studies of novel cell selective antimicrobial peptides with model membranes and *E. coli* ATCC 11775. *Biochim. Biophys. Acta* 1798, 1864–1875. doi: 10.1016/j.bbame.2010.06.016
- Koradi, R., Billeter, M., and Wüthrich, K. (1996). MOLMOL: a program for display and analysis of macromolecular structures. *J. Mol. Graph.* 14, 51–55. doi: 10.1016/0263-7855(96)00009-4
- Kumar, A., Ernst, R. R., and Wüthrich, K. (1980). A two-dimensional nuclear Overhauser enhancement (2D NOE) experiment for the elucidation of complete proton-proton cross-relaxation networks in biological macromolecules. *Biochem. Biophys. Res. Commun.* 95, 1–6. doi: 10.1016/0006-291X(80)90695-6
- Kuprin, S., Graslund, A., Ehrenberg, A., and Koch, M. H. (1995). Nonideality of water-hexafluoropropanol mixtures as studied by X-ray small angle scattering. *Biochem. Biophys. Res. Commun.* 217, 1151–1156. doi: 10.1006/bbrc.1995.2889
- Laskowski, R. A., Rullmann, J. A., MacArthur, M. W., Kaptein, R., and Thornton, J. M. (1996). AQUA and PROCHECK-NMR: programs for checking the quality of protein structures solved by NMR. *J. Biomol. NMR* 8, 477–486. doi: 10.1007/BF00228148
- Lira, S. A., Zalamea, P., Heinrich, J. N., Fuentes, M. E., Carrasco, D., Lewin, A. C., et al. (1994). Expression of the chemokine N51/KC in the thymus and epidermis of transgenic mice results in marked infiltration of a single class of inflammatory cells. *J. Exp. Med.* 180, 2039–2048. doi: 10.1084/jem.180.6.2039
- Malanovic, N., and Lohner, K. (2016). Gram-positive bacterial cell envelopes: the impact on the activity of antimicrobial peptides. *Biochim. Biophys. Acta* 1858, 936–946. doi: 10.1016/j.bbame.2015.11.004
- Malmsten, M. (2016). Interactions of antimicrobial peptides with bacterial membranes and membrane components. *Curr. Top. Med. Chem.* 16, 16–24. doi: 10.2174/1568026615666150703121518
- Mathews, C. J., Weston, V. C., Jones, A., Field, M., and Coakley, G. (2010). Bacterial septic arthritis in adults. *Lancet* 375, 846–855. doi: 10.1016/S0140-6736(09)61595-6
- Matsuzawa, T., and Ikarashi, Y. (1979). Haemolysis of various mammalian erythrocytes in sodium chloride, glucose and phosphate-buffer solutions. *Lab. Anim.* 13, 329–331. doi: 10.1258/002367797980943297
- Mookherjee, N., and Hancock, R. E. (2007). Cationic host defence peptides: innate immune regulatory peptides as a novel approach for treating infections. *Cell. Mol. Life Sci.* 64, 922–933. doi: 10.1007/s00018-007-6475-6
- Nizet, V. (2006). Antimicrobial peptide resistance mechanisms of human bacterial pathogens. *Curr. Issues Mol. Biol.* 8, 11–26.
- Othon, C. M., Kwon, O. H., Lin, M. M., and Zewail, A. H. (2009). Solvation in protein (un)folding of melittin tetramer-monomer transition. *Proc. Natl. Acad. Sci. U.S.A.* 106, 12593–12598. doi: 10.1073/pnas.0905967106
- Overhage, J., Campisano, A., Bains, M., Torfs, E. C., Rehm, B. H., and Hancock, R. E. (2008). Human host defense peptide LL-37 prevents bacterial biofilm formation. *Infect. Immun.* 76, 4176–4182. doi: 10.1128/IAI.00318-08
- Park, K. H., Nan, Y. H., Park, Y., Kim, J. I., Park, I. S., Hahm, K. S., et al. (2009). Cell specificity, anti-inflammatory activity, and plausible bactericidal mechanism of designed Trp-rich model antimicrobial peptides. *Biochim. Biophys. Acta* 1788, 1193–1203. doi: 10.1016/j.bbame.2009.02.020
- Resende, J. M., Moraes, C. M., Prates, M. V., Cesar, A., Almeida, F. C., Mundim, N. C., et al. (2008). Solution NMR structures of the antimicrobial peptides phyloseptin-1, -2, and -3 and biological activity: the role of charges and hydrogen bonding interactions in stabilizing helix conformations. *Peptides* 29, 1633–1644. doi: 10.1016/j.peptides.2008.06.022
- Sachs, D., Coelho, F. M., Costa, V. V., Lopes, F., Pinho, V., Amaral, F. A., et al. (2011). Cooperative role of tumour necrosis factor- α , interleukin- β and neutrophils in a novel behavioural model that concomitantly demonstrates articular inflammation and hypernociception in mice. *Br. J. Pharmacol.* 162, 72–83. doi: 10.1111/j.1476-5381.2010.00895.x
- Santos, D. M., Reis, P. V., and Pimenta, A. M. C. (2016). “Antimicrobial peptides in spider venoms,” in *Spider Venoms*, eds P. Gopalakrishnakone, G. A. Corzo, M. E. de Lima, and E. Diego-García (Dordrecht: Springer), 361–377.
- Santos, D. M., Verly, R. M., Piló-Veloso, D., de Maria, M., de Carvalho, M. A., Cisalpino, P. S., et al. (2010). LyeTx I, a potent antimicrobial peptide from the venom of the spider *Lycosa erythrognatha*. *Amino Acids* 39, 135–144. doi: 10.1007/s00726-009-0385-x
- Schanda, P., and Brutscher, B. (2005). Very fast two-dimensional NMR spectroscopy for real-time investigation of dynamic events in proteins on the time scale of seconds. *J. Am. Chem. Soc.* 127, 8014–8015. doi: 10.1021/ja051306e
- Schwieters, C. D., Kuszewski, J. J., Tjandra, N., and Clore, G. M. (2003). The Xplor-NIH NMR molecular structure determination package. *J. Magn. Reson.* 160, 65–73. doi: 10.1016/S1090-7807(02)00014-9
- Sharff, K. A., Richards, E. P., and Townes, J. M. (2013). Clinical management of septic arthritis. *Curr. Rheumatol. Rep.* 15:332. doi: 10.1007/s11926-013-0332-4
- Shen, Y., Delaglio, F., Cornilescu, G., and Bax, A. (2009). TALOS+: a hybrid method for predicting protein backbone torsion angles from NMR chemical shifts. *J. Biomol. NMR* 44, 213–223. doi: 10.1007/s10858-009-9332-z
- Tremblay, M. L., Banks, A. W., and Rainey, J. K. (2010). The predictive accuracy of secondary chemical shifts is more affected by protein secondary structure than

- solvent environment. *J. Biomol. NMR* 46, 257–270. doi: 10.1007/s10858-010-9400-5
- Urech, D. M., Feige, U., Ewert, S., Schlosser, V., Ottiger, M., Polzer, K., et al. (2010). Anti-inflammatory and cartilage-protecting effects of an intra-articularly injected anti-TNF[alpha] single-chain Fv antibody (ESBA105) designed for local therapeutic use. *Ann. Rheum. Dis.* 69, 443–449. doi: 10.1136/ard.2008.105775
- Verly, R. M., de Moraes, C. M., Resende, J. M., Aisenbrey, C., Bemquerer, M. P., Piló-Veloso, D., et al. (2009). Structure and membrane interactions of the antibiotic peptide dermadistinctin K by multidimensional solution and oriented 15N and 31P solid-state NMR spectroscopy. *Biophys. J.* 96, 2194–2203. doi: 10.1016/j.bpj.2008.11.063
- Verly, R. M., Resende, J. M., Junior, E. F., de Magalhaes, M. T., Guimaraes, C. F., Munhoz, V. H., et al. (2017). Structure and membrane interactions of the homodimeric antibiotic peptide homotarsinin. *Sci. Rep.* 7:40854. doi: 10.1038/srep40854
- Voievoda, N., Schulthess, T., Bechinger, B., and Seelig, J. (2015). Thermodynamic and biophysical analysis of the membrane-association of a histidine-rich peptide with efficient antimicrobial and transfection activities. *J. Phys. Chem. B* 119, 9678–9687. doi: 10.1021/acs.jpcc.5b04543
- Wang, G., Epand, R. F., Mishra, B., Lushnikova, T., Thomas, V. C., Bayles, K. W., et al. (2012). Decoding the functional roles of cationic side chains of the major antimicrobial region of human cathelicidin LL-37. *Antimicrob. Agents Chemother.* 56, 845–856. doi: 10.1128/AAC.05637-11
- Weston, V. C., Jones, A. C., Bradbury, N., Fawthrop, F., and Doherty, M. (1999). Clinical features and outcome of septic arthritis in a single UK Health District 1982–1991. *Ann. Rheum. Dis.* 58, 214–219. doi: 10.1136/ard.58.4.214
- WHO (2014). *Antimicrobial Resistance: Global Report on Surveillance*. Geneva: WHO.
- Wiegand, I., Hilpert, K., and Hancock, R. E. (2008). Agar and broth dilution methods to determine the minimal inhibitory concentration (MIC) of antimicrobial substances. *Nat. Protoc.* 3, 163–175. doi: 10.1038/nprot.2007.521
- Willker, W., Leibfritz, D., Kerssebaum, R., and Bermel, W. (1993). Gradient selection in inverse heteronuclear correlation spectroscopy. *Magn. Reson. Chem.* 31, 287–292. doi: 10.1002/mrc.1260310315
- Wishart, D. S., Sykes, B. D., and Richards, F. M. (1992). The chemical shift index: a fast and simple method for the assignment of protein secondary structure through NMR spectroscopy. *Biochemistry* 31, 1647–1651. doi: 10.1021/bi00121a010
- Yang, L., Harroun, T. A., Weiss, T. M., Ding, L., and Huang, H. W. (2001). Barrel-stave model or toroidal model? A case study on melittin pores. *Biophys. J.* 81, 1475–1485. doi: 10.1016/S0006-3495(01)75802-X
- Zanin, L. P., de Araujo, A. S., Juliano, M. A., Casella, T., Nogueira, M. C., and Ruggiero Neto, J. (2016). Effects of N-terminus modifications on the conformation and permeation activities of the synthetic peptide L1A. *Amino Acids* 48, 1433–1444. doi: 10.1007/s00726-016-2196-1

Conflict of Interest Statement: The authors declare that the research was conducted in the absence of any commercial or financial relationships that could be construed as a potential conflict of interest.

Copyright © 2018 Reis, Boff, Verly, Melo-Braga, Cortés, Santos, Pimenta, Amaral, Resende and de Lima. This is an open-access article distributed under the terms of the Creative Commons Attribution License (CC BY). The use, distribution or reproduction in other forums is permitted, provided the original author(s) and the copyright owner are credited and that the original publication in this journal is cited, in accordance with accepted academic practice. No use, distribution or reproduction is permitted which does not comply with these terms.